



HAL
open science

A robust alternative to assessing three-dimensional relative enamel thickness for the use in taxonomic assessment

Zhixing Yi, Wei Liao, Clément Zanolli, Wei Wang

► **To cite this version:**

Zhixing Yi, Wei Liao, Clément Zanolli, Wei Wang. A robust alternative to assessing three-dimensional relative enamel thickness for the use in taxonomic assessment. *American Journal of Physical Anthropology*, 2020, 10.1002/ajpa.24187 . hal-03040304

HAL Id: hal-03040304

<https://hal.science/hal-03040304v1>

Submitted on 4 Dec 2020

HAL is a multi-disciplinary open access archive for the deposit and dissemination of scientific research documents, whether they are published or not. The documents may come from teaching and research institutions in France or abroad, or from public or private research centers.

L'archive ouverte pluridisciplinaire **HAL**, est destinée au dépôt et à la diffusion de documents scientifiques de niveau recherche, publiés ou non, émanant des établissements d'enseignement et de recherche français ou étrangers, des laboratoires publics ou privés.

A robust alternative to assessing three - dimensional relative enamel thickness for the use in taxonomic assessment

Zhixing Yi¹, Wei Liao^{1,2}, Clément Zanolli³, and Wei Wang^{2,4*}

¹ School of Earth Sciences, China University of Geosciences, Wuhan, China.

² Anthropology Museum of Guangxi, Nanning, China.

³ Laboratoire PACEA, UMR 5199 CNRS, Université de Bordeaux, Pessac, France.

⁴ Institute of Cultural Heritage, Shandong University, Qingdao, China.

*Corresponding author: Wei Wang (wangw@sdu.edu.cn)

Abstract

Objective: Three - dimensional relative enamel thickness (3DRET) is important for assessing hypotheses about taxonomy, phylogeny, and dietary reconstruction for primates. However, its weaknesses have not been thoroughly investigated. Here, we analyze its weaknesses and propose an index aiming at better taxonomic discrimination.

Materials and Methods: The dimensionless 3D index, ratio of enamel - thickness to dentine - thickness (3DRED), which is defined as the cubic root of the ratio of 3D average enamel thickness (3DAET) to 3D average dentine thickness (3DADT), is proposed here. To compare 3DRET and 3DRED and their sensitivity to voxel size, a fossil orangutan molar was scanned 14 times with different resolutions ranging from 10 to 50 μm . Enamel thickness analysis was carried out for each resultant digital model. In addition, enamel thickness measurements of 179 mandibular permanent molars (eight genera) were analyzed, followed by investigating the relationship between 3DRET and 3DAET and between 3DRED and 3DAET.

Results: Regarding sensitivity, 3DRED is more robust than 3DRET. In addition, 3DRET is correlated with 3DAET by linear curve with regression coefficients approximating or larger than 0.8 in most cases, while 3DRED shows less correlation with 3DAET. Furthermore, there are clear separations between different taxa in the bivariate plot of 3DRED against 3DAET, indicative of the taxonomic value of 3DRED.

Conclusion: Under certain conditions, 3DRED promises to be a robust and reliable alternative to 3DRET in taxonomic study.

KEYWORDS

enamel/dentine thickness ratio, hominid teeth, relative enamel thickness, taxonomic assessment, voxel size sensibility.

Primate enamel thickness variation stems from an evolutionary interplay between functional/adaptive constraints (ecology) and strict control mechanisms of the morphogenetic program (Horvath et al., 2014; Kelley & Swanson, 2008; Simmer et al., 2010; Vogel et al., 2008). This mineralized dental tissue appears to respond relatively quickly in evolutionary time to dietary/ecological changes (Grine & Daegling, 2017; Hlusko, Suwa, Kono, & Mahaney, 2004; Le Luyer & Bayle, 2017), thus being prone to homoplasy (Smith, Olejniczak, et al., 2012). Commonly

40 used to infer durophagy and considered as a proxy of the dietary niches exploited by extinct species
41 (e.g., Constantino et al., 2011, 2012; Lucas, Constantino, Wood, & Lawn, 2008; Martin, Olejniczak,
42 & Maas, 2003; Schwartz, 2000; Teaford, 2007; Teaford & Ungar, 2015; Vogel et al., 2008), it is
43 intimately related to dietary abrasiveness and selectively responsive to lifetime dental wear
44 resistance (Pampush et al., 2013; Rabenold & Pearson, 2011). Despite some degree of plasticity of
45 enamel thickness, it is still considered an important indicator of taxonomy, phylogeny, and dietary
46 signals in extant and fossil primates (e.g., Alba et al., 2013; Kono, Zhang, Jin, Takai, & Suwa, 2014;
47 Lockey, Alemseged, Hublin, & Skinner, 2020; Macchiarelli, Bayle, Bondioli, Mazurier, & Zanolli,
48 2013; Pan et al., 2016; Skinner, Alemseged, Gaunitz, & Hublin, 2015; Smith, Tafforeau, Pouech, &
49 Begun, 2019; Thiery, Guy, & Lazzari, 2019; Thiery, Lazzari, Ramdarshan, & Guy, 2017; Zanolli et
50 al., 2017; Zanolli, Biglari, et al., 2019; Zanolli, Kullmer, et al., 2019).

51
52 Since the pioneering studies of Gantt (1977), Kay (1981), and Martin (1983, 1985), enamel
53 thickness has been investigated in various ways. In early works, enamel thickness was measured on
54 physical ground section of tooth (e.g., Andrews & Martin, 1991; Beynon & Wood, 1986; Dean &
55 Schrenk, 2003; Schwartz, 2000; Smith, Martin, & Leakey, 2003) or virtual section of digital tooth
56 model acquired via conventional computed tomography (CT) instruments (e.g., Conroy & Vannier,
57 1991; Schwartz, Thackeray, Reid, & van Reenan, 1998; Shimizu, 2002). The former approach is
58 destructive, limiting both intrataxon and intertaxon comparisons among sufficiently large samples.
59 Besides, the manually cut ground section is inevitably oblique to the ideal plane (a plane passing
60 through the mesial cusp tips and perpendicular to the cervix plane), potentially leading to biased
61 result (Olejniczak, 2006). For conventional CT, its scanning voxel size is generally at the scale of
62 100 μm and the voxel size is not small enough to reconstruct a precise digital substitute of tooth
63 sample. Considering these situations, the advent of micro - CT (subsequently attracted widespread
64 interests owing to its high resolution, thus allowing both nondestructive access to the details of
65 three - dimensional (3D) tooth internal structural organization and precise quantitative analyses of
66 bidimensional (2D) and 3D enamel thickness (Benazzi et al., 2014; Feeney et al., 2010; Kono, 2004;
67 Macchiarelli et al., 2004; Macchiarelli, Bondioli, & Mazurier, 2008; Macchiarelli, Mazurier,
68 Illerhaus, & Zanolli, 2009; Olejniczak, 2006; Tafforeau, 2004).

69
70 During the past two decades, an increasing number of micro - CT - based studies were presented
71 to elucidate and compare enamel thickness pattern in taxonomically broad samples, including fossil
72 hominins (e.g., Becam & Chevalier, 2019; Fornai et al., 2014; Olejniczak, Smith, Feeney, et al.,
73 2008; Olejniczak, Smith, Skinner, et al., 2008; Skinner et al., 2015; Smith, Harvati, et al., 2009;
74 Smith, Olejniczak, et al., 2009; Smith, Olejniczak, et al., 2012; Zanolli, Biglari, et al., 2019), fossil
75 hominoids (e.g., Alba, Fortuny, & Moya - Sola, 2010; Kono et al., 2014; Olejniczak, Smith, Wang,
76 et al., 2008; Smith et al., 2019; Zanolli et al., 2016; Zanolli, Kullmer, et al., 2019), extant hominoids
77 (e.g., Kono & Suwa, 2008; Olejniczak, Tafforeau, Feeney, & Martin, 2008; Smith et al., 2011; Smith,
78 Kupczik, Machanda, Skinner, & Zermeno, 2012), and extant cercopithecoids (e.g., Beaudet et al.,
79 2016; Kato et al., 2014; Olejniczak, Tafforeau, et al., 2008). Moreover, efforts have been extended
80 from 2D to 3D analysis (e.g., Buti et al., 2017; Guy, Lazzari, Gilissen, & Thiery, 2015; Hu & Zhao,
81 2015; Martín Francés et al., 2018; Pan et al., 2016; Zanolli, Kullmer, et al., 2019; Zhang & Zhao,
82 2013). Other than the classic enamel thickness indices like the average enamel thickness (AET) and
83 relative enamel thickness (RET) (Kono, 2004; Martin, 1985), attempts were made to develop

84 derivatives like the lateral RET to study worn teeth (e.g., Benazzi et al., 2011; Kono & Suwa, 2008;
85 Toussaint et al., 2010; Zanolli et al., 2018). Most recently, a novel metric was proposed, the absolute
86 crown strength estimated on 2D sections, to estimate tooth crown resistance to fracture (Schwartz,
87 McGrowsky, & Strait, 2020).

88

89 Despite the flexibility associated with micro - CT technology, it is very important to bear in mind
90 that digital model is an approximation to the studied sample, and its quality is controlled by the
91 voxel size (spatial resolution). Consequently, some elements (e.g., dentine horns) would lose details,
92 if voxel size is too large. Olejniczak (2006) has noted that the model quality is reduced when spatial
93 resolution is low. Nevertheless, a further study to investigate the effect of voxel size on enamel
94 thickness indices is missing in his study or in others. Furthermore, an increasing number of studies
95 have applied multivariable - based method (e.g., adjusted Z - score statistics, Maureille, Rougier,
96 Houët, & Vandermeersch, 2001; Scolan, Santos, Tillier, Maureille, & Quintard, 2012) to indicate
97 the taxonomic status for given samples. To ensure the effectiveness and accuracy of multivariable -
98 based statistics, it is better to avoid linear correlations among variables. 3DAET and 3DRET are
99 two indices widely adopted in multivariable - based statistics and hence it is significant to ascertain
100 their relationship. Given the above reasons, we test how much 3DRET and 3DAET are sensitive to
101 voxel size of the microtomographic scans in this contribution. We then test the correlation between
102 3DRET and 3DAET. In parallel to these tests, we introduce an analogue to 3DRET, the ratio of
103 enamel - thickness to dentine - thickness (3DRED). For this index, its sensitivity to voxel size and
104 its correlation with 3DAET were also analyzed.

105

106 2 MATERIALS AND METHODS

107 2.1 An analogue to 3DRET

108 The definitions of 3DAET and 3DRET are shown in Equations (1) and (2), respectively.

$$109 \quad 3DAET = \frac{V_e}{S_{edj}} \quad (1)$$

$$110 \quad 3DRET = 100 \times \frac{3DAET}{\sqrt[3]{V_{cdp}}} = 100 \times \frac{V_e}{S_{edj} \sqrt[3]{V_{cdp}}} \quad (2)$$

111 where V_e is the enamel volume (mm³) and V_{cdp} is the coronal dentine volume (including the
112 volume of the pulp cavity) in mm³. S_{edj} is the enamel–dentine junction (EDJ) surface area (mm²).
113 The analogue to 3DRET that we developed here is 3DRED. This dimensionless index is defined as
114 the cubic root of the ratio of 3DAET to 3DADT, which is expressed as

$$115 \quad 3DRED = 10 \times \left(\frac{3DAET}{3DADT} \right)^{\frac{1}{3}} \quad (3)$$

116 The ratio is multiplied by 10 for ease interpretation. For the 3D average dentine thickness (3DADT,
117 mm), the equation is as follows:

$$118 \quad 3DADT = \frac{V_{cdp}}{S_{edj}} \quad (4)$$

119 3DADT describes the average thickness from EDJ surface to cervical plane. Substituting the

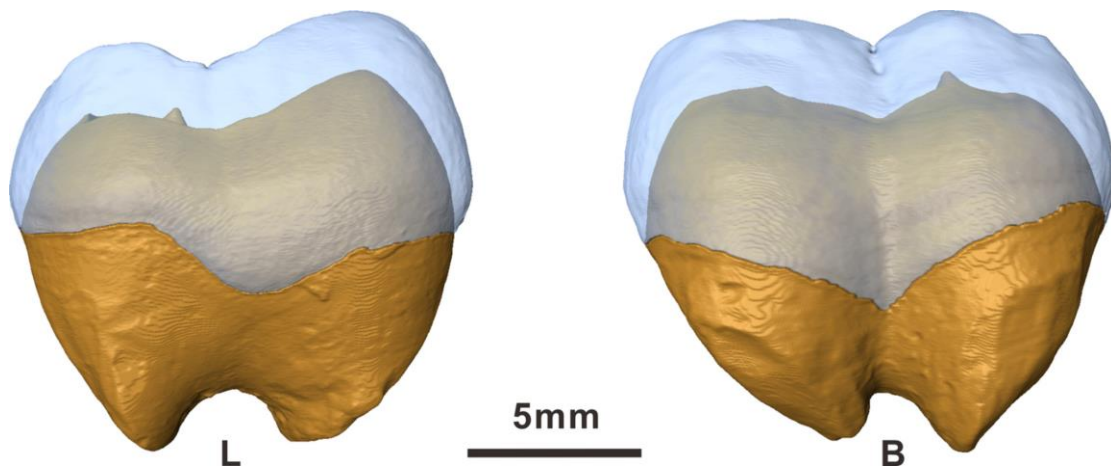
120 expressions of 3DAET (Equation (1)) and 3DADT (Equation (4)) into Equation (3) yields simpler
121 expression of 3DRED, as shown in the following.

$$3DRED = 10 \times \left(\frac{3DAET}{3DADT} \right)^{\frac{1}{3}} = 10 \times \left(\frac{V_e / V_{cdp}}{S_{edj} / S_{edj}} \right)^{\frac{1}{3}} = 10 \times \left(\frac{V_e}{V_{cdp}} \right)^{\frac{1}{3}} \quad (5)$$

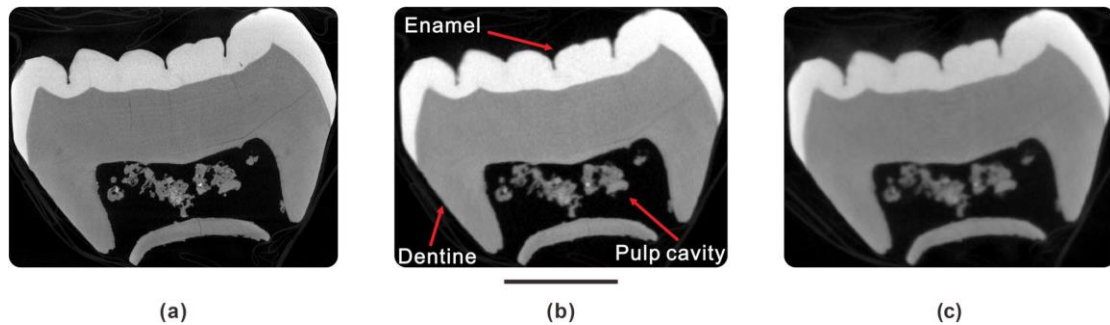
122
123 From Equation (5), it can be seen that 3DRED only depends on two basic variables cubic root of V_e
124 and cubic root of V_{cdp} in essential. One could be curious about why we extracted the cubic root,
125 since the ratio of enamel volume to coronal dentine volume (V_e/V_{cdp}) has been dimensionless.
126 Indeed, extracting the cubic root will not change the ability of 3DRED to spot differences between
127 taxa. The significance is that extracting the cubic root makes the basic variables involved in 3DRED
128 be linear scale (1D, cubic root of V_e and cubic root of V_{cdp}), which generally shows less sensitive
129 to spatial resolution compared to higher dimensional parameters like enamel volume (3D) and
130 coronal dentine volume (3D).

131 132 2.2 Materials and methods for assessing sensitivity

133 To assess the effect of voxel size on enamel thickness measurements, a nearly unworn Pleistocene
134 orangutan lower third molar (specimen NX - C2 - 9, Figure 1) from the site of Naxian cave,
135 Guangxi, China, was selected for study due to the following reasons. First, this specimen bears
136 complete sinuous cervical line (Figure 1). Therefore, all routine methods for analyzing enamel
137 thickness can be adopted. Second, no apparent diagenesis signals and fractures are observed in this
138 molar, so that the contrast between enamel and dentine in Micro - CT images is obvious (Figure 2)
139 and hence manual correction, which may bring in operator - dependent differences, is minimized.
140



141
142 FIGURE 1. Virtual three - dimensional (3D) reconstruction of the fossil Pongo molar with a voxel
143 size of 20 μm . The enamel is rendered in semitransparency, showing the underlying enamel-dentine
144 junction (EDJ) surface. L: lingual, B: buccal.
145



146 (a) (b) (c)
 147 FIGURE 2. Slices from image stacks with voxel size of (a) 10, (b) 29, and (c) 50 μm , respectively.
 148 Scale bar is 5 mm

149
 150 This molar was scanned 14 times with a nanoVoxel4000 Micro - CT (Sanying Precision Instruments,
 151 Tianjin, China). Only the distance between X - ray source and object and the distance between X -
 152 ray source and detector differed for each acquisition (Supplementary Material Table 1). After
 153 scanning, volume dataset was reconstructed with VoxelStudio Recon (Sanying Precision
 154 Instruments) and 14 image stacks with isometric voxel size ranging from 10 to 50 μm were obtained
 155 accordingly (Supplementary Material Table 1). These image stacks were segmented using
 156 watershed algorithm in Avizo 8.0 and surface renderings were generated with constrained
 157 smoothing algorithm (kernel size: 3). The resultant digital models were imported in Geomagic
 158 Design X.2016 to create dental crown and measure dental metrics (e.g., enamel volume).

159
 160 Following Benazzi et al. (2014), three different protocols were generally used to separate the crown
 161 from the roots (denoted by 3D - a, 3D - b, and 3D - c, respectively). The main difference among
 162 these methods lies in the definition of the reference plane or surface that separates the crown from
 163 the roots. In 3D - a, a best fitting plane is produced according to the cervical line path (Tafforeau,
 164 2004). In 3D - b, the cervical line is used to create a digitized spline curve. After that, the curve is
 165 interpolated into a smooth surface (Benazzi et al., 2014). In 3D - c, the most apical plane (Plane A)
 166 containing a continuous ring of enamel at the cervix is first located, and parallel to that plane,
 167 another plane that contains the most apical enamel extension is further defined as Plane B. The final
 168 cervical plane is the average plane between Planes A and B (Olejniczak, 2006). Once the target
 169 plane or surface has been created, the crown is separated from the roots and 3D measurements
 170 (enamel volume, EDJ surface area, and dentine volume) are performed. The 3DAET, 3DRET, and
 171 3DRED are then calculated in accordance with Equations (1)–(3)–(1)–(3), respectively (Kono, 2004;
 172 Olejniczak, 2006; Tafforeau, 2004).

173
 174 All routine protocols mentioned above were tested here on the fossil Pongo molar. Besides, 3D
 175 enamel thickness distribution was analyzed through the “surface distance” module in Avizo 8.0. All
 176 postprocessing, including segmentation, digitizing cervical line, and determining cervical
 177 plane/surface were done by a single observer to avoid interobserver variation. In addition, the
 178 measurements have been repeated three times over a period of 6 months. Intraobserver variation
 179 (calculated as the maximum deviation from the mean of three measurements) was less than 2% for
 180 3DAET, 3DRET, and 3DRED.

181 182 2.3 Materials and methods for assessing correlation between enamel thickness variables

183 Additionally, to test the newly introduced 3DRED index, we used a sample consisting of 179
 184 mandibular permanent first, second, and third molars of various fossil and extant hominid taxa as
 185 listed in Table 1. Detailed information on these samples are documented in Supplementary Material
 186 Table 2. Dental measurements of some molars (n = 146) were directly cited from references and we
 187 only calculated 3DRED according to their results. Other molars (n = 33) are from open - source
 188 database, including NESPOS, ESRF, and Morphosource. These original Micro - CT data were
 189 segmented and then converted into surface model following the methods mentioned above. Dental
 190 crown was separated in line with the protocol 3D - c (Olejniczak, 2006). After that, dental
 191 measurements were performed in Geomagic Design X.2016.

192

193 TABLE 1. Dental material included in this study

Taxon	M1	M2	M3	Total	Source^a
<i>Hylobates</i> . sp. (extant)	6	6	3	15	1, 7
<i>Symphalangus syndactylus</i>	5	9	3	17	1
<i>Pongo</i> . sp. (extant)	6	9	7	22	1, 2
<i>Gorilla gorilla</i>	4	4	0	8	1
<i>Pan troglodytes</i>	10	9	7	26	1, 7
Neanderthals	16	6	9	31	3, 4, 7, 8
Modern humans	15	12	11	38	1, 5, 9
<i>Paranthropus robustus</i>	6	8	8	22	5, 6
Total	68	63	48	179	

194 ^aSource: 1 - Olejniczak, Tafforeau, et al., 2008; 2 - Zanolli, Kullmer, et al., 2019; 3 - Olejniczak,
 195 Smith, Feeney, et al., 2008; 4 - Becam & Chevalier, 2019; 5 - Pan et al., 2016; 6 - Olejniczak,
 196 Smith, Skinner, et al., 2008; 7 - ESRF, 2020; 8 - NESPOS Database, 2020; 9 - Morphosource,
 197 2020.

198

199 3 RESULTS AND DISCUSSION

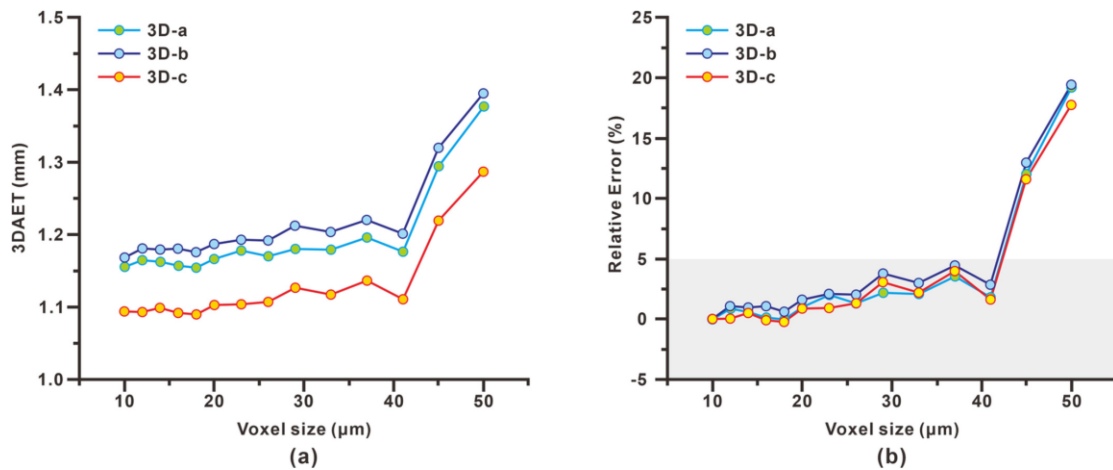
200 3.1 Sensitivity of enamel thickness indices to voxel size

201 The raw data of 3D dental measurements for the fossil Pongo (mesiodistal and buccolingual
 202 diameters are 14.34 and 12.22 mm, respectively) are provided in Supplementary Material Table 3.
 203 Detailed analysis is summarized below.

204

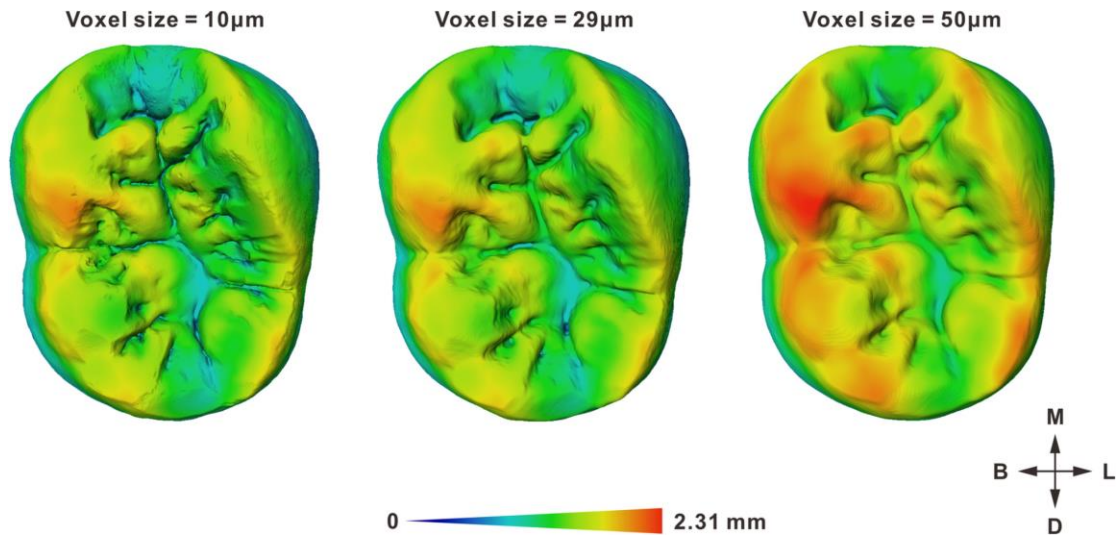
205 When using Micro - CT scanning to assess enamel thickness, the final voxel size may vary
 206 depending on the size of the sample. However, for the same sample, depending if the voxel size is
 207 small or large, differences in enamel thickness measurements may be noted. As we can see in Figure
 208 3a, 3DAET will not change significantly when the voxel size is smaller than 40 μm , while with a
 209 voxel size that is larger than 40 μm , the result deviate drastically from the 10 μm value. In other

210 words, substantive details have been revealed under the condition of voxel size smaller than 40 μm
 211 for calculating 3DAET, but the digital model reconstructed at voxel size larger than 40 μm cannot
 212 be taken as a reasonable representative of the study molar. In this work, the result measured at 10
 213 μm digital model is taken as the reference. Relative error (calculated as the difference from the result
 214 at 10 μm voxel size) for each scan is provided in Figure 3b. The maximum relative error can reach
 215 up to $\sim 20\%$ at voxel size of 50 μm , highlighting the significance of selecting an appropriate
 216 resolution. If voxel size is smaller than 40 μm , all relative errors are less than 5%, indicating that
 217 3DAET estimates are reliable and comparable under this condition.
 218



219
 220 FIGURE 3. (a) Three - dimensional average enamel thickness (3DAET) results at different voxel
 221 sizes and (b) their corresponding relative errors. Here and later, light shading zone marks the slight
 222 deviation with relative error ranging from -5 to 5% .
 223

224 Figure 4 shows the enamel thickness map at different voxel size. The first two figures (left and
 225 middle) display similar distribution pattern and rich details, since both were reconstructed from
 226 image stacks with smaller voxel size (10 and 29 μm , respectively). However, the third one (right)
 227 shows evident discrepancy, with much thicker enamel around the cusp tips and occlusal ridges,
 228 indicating that enamel thickness is clearly overestimated when the fossil Pongo molar is
 229 reconstructed with 50 μm voxel size. This finding is consistent with the result shown in Figure 3.
 230



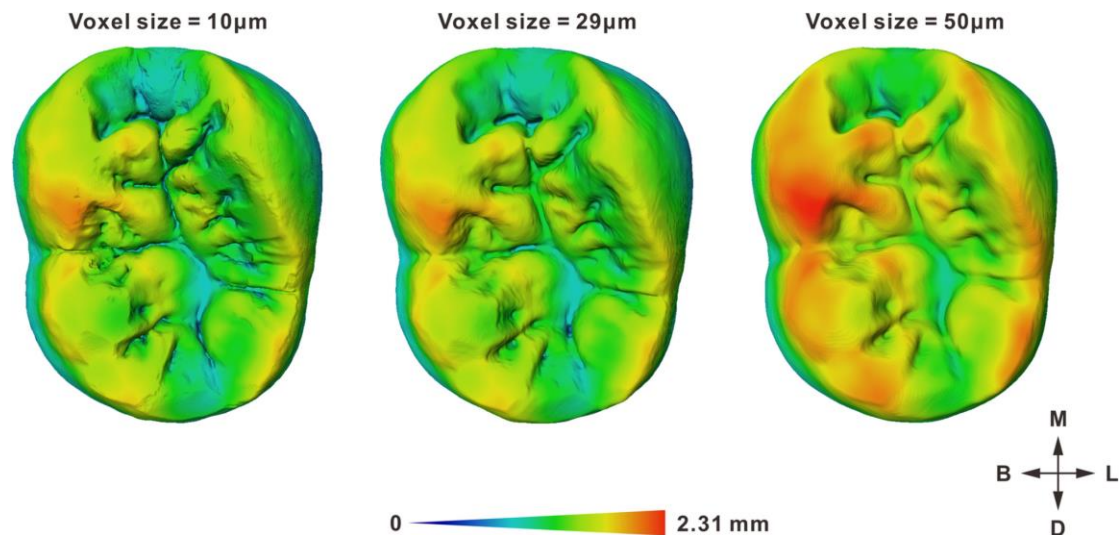
231

232 FIGURE 4. Three - dimensional (3D) enamel thickness distributions at voxel size of 10 μm (left),
 233 29 μm (middle), and 50 μm (right). M: mesial, B: buccal, D: distal, L: lingual.

234

235 Figure 5 shows that 3DRET is positively correlated with voxel size. To obtain a reliable 3DRET for
 236 this fossil Pongo molar, the critical voxel size is about 30 μm (Figure 5b), which is smaller than that
 237 for 3DAET (40 μm) (Figure 3b). Compared to 3DRET, 3DRED is more robust to voxel size (Figure
 238 5a). For the former, the maximum relative error can reach up to $\sim 14\%$ (Figure 5b), while for the
 239 latter, relative errors are less than 5% in most cases and the maximum is about 5% (Figure 5c).
 240 Among the three enamel thickness indices (3DAET, 3DRET, and 3DRED), 3DRED is the most
 241 robust one and 3DAET is more robust than 3DRET. Micro - CT volume data is an approximation
 242 to the studied sample, somewhat like using Legos to build the target. Therefore, the linear
 243 relationship between 3DRET and voxel size is mainly due to the voxelization nature of Micro - CT
 244 but not to the tooth morphology. The sensitivity of 3DRET to voxel size thus most likely exists in
 245 other taxa and other kind of teeth, meaning that discrepancies could occur between specimens
 246 scanned at different resolutions. For instance, Benazzi et al. (2014) scanned a gorilla skull and
 247 analyzed the enamel thickness of a lower molar. Their result showed that 3DRET is 14.12. However,
 248 Olejniczak, Tafforeau, et al. (2008) systematically analyzed enamel thickness in a relatively larger
 249 sample of gorilla mandibular molars ($n = 8$) and the mean 3DRET is 9.40 (ranging from 7.12 to
 250 11.74). Although the two research groups have scanned different gorilla specimens and there could
 251 exist interspecific variations, this discrepancy may well lie with the voxel size difference between
 252 them since in the study by Benazzi et al. (2014), the entire skull was scanned at a voxel size of
 253 61 μm , while in Olejniczak, Tafforeau, et al. (2008), the molars were scanned separately at a voxel
 254 size of 30.3 μm .

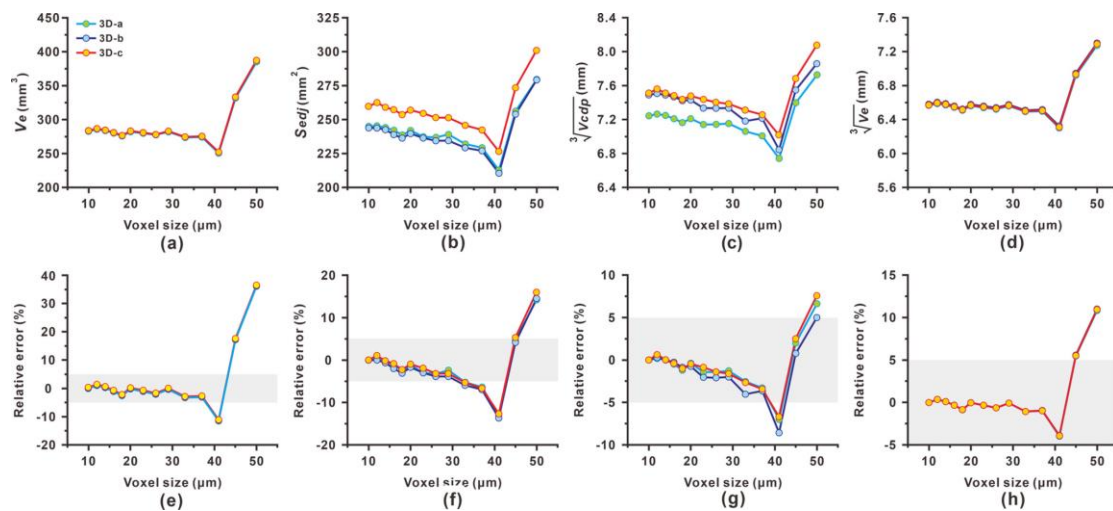
255



256
 257 FIGURE 5. (a) Three - dimensional relative enamel thickness (3DRET) and ratio of enamel -
 258 thickness to dentine - thickness (3DRED) at different voxel sizes and the relative errors of (b)
 259 3DRET and (c) 3DRED. See caption of Figure 3 for graph description.

260
 261 Why 3DAET, 3DRET, and 3DRED present diverse sensitivity patterns to voxel size? To interpret
 262 this disparity, we shift attention to the effect of voxel size on enamel volume (Figure 6a), EDJ
 263 surface area (Figure 6b), cubic root of coronal dentine volume (Figure 6c) and cubic root of enamel
 264 volume (Figure 6d), since these basic parameters are involved in the calculation of enamel thickness
 265 indices. It can be seen that all parameters will be affected by the voxel size (Figure 6a–d). And there
 266 exists threshold voxel size for these parameters. When voxel size is smaller than the threshold, these
 267 parameters show slight sensitive to the fluctuation of spatial resolution. Yet if voxel size is larger
 268 than the threshold value, relative error is getting larger. Here and later, our analysis is mainly focused
 269 on the sensitivity patterns of enamel thickness indices when voxel size is larger than the threshold.
 270 A significant finding is that the higher the parameter dimension is, the larger the maximum error is.
 271 In specific, the maximum errors of V_e (3D), S_{edj} (2D), cubic root of V_{cdp} (1D), and cubic root of
 272 V_e (1D) are about 35, 15, 8, and 11%, respectively (Figure 6e–h). 3DAET is the ratio of V_e to S_{edj} ,
 273 and the variation of S_{edj} compensates to the variation of V_e to some extent since these two
 274 parameters show similar trend (getting larger) after 40 μm . However, the S_{edj} variation cannot
 275 completely offset the V_e variation, because these two parameters are of different dimensions and
 276 thus show varying sensitivity to voxel size (Figure 6e,f). Compared to 3DAET, 3DRET needs
 277 additional parameter: cubic root of V_{cdp} . Consequently, the sensitivity pattern of 3DRET to voxel
 278 size is different from that of 3DAET. 3DRET relates to the ratio of 3DAET to cubic root of V_{cdp}
 279 (Equation (2)). When voxel size is smaller than the threshold, 3DAET shows slight positive trend
 280 with the increasing voxel size (Figure 3a) while cubic root of V_{cdp} presents slight negative
 281 relationship with voxel size (Figure 6c), both leading to slightly overestimated 3DRET (Figure 5a).
 282 When voxel size is larger than the threshold, cubic root of V_{cdp} is also getting larger. However, the
 283 variation of cubic root of V_{cdp} (1D) cannot completely counterweigh the variations of V_e (3D) and
 284 S_{edj} (2D), so that 3DRET still show moderate relative error at larger voxel size (e.g., 50 μm). Unlike
 285 3DAET and 3DRET where basic parameters (V_e , S_{edj} , and cubic root of V_{cdp}) are of different
 286 dimensions, 3DRED is essentially affected by two comparable parameters with the same dimension
 287 (1D, cubic root of V_e , and cubic root of V_{cdp}). Low - dimensional parameters show less sensitivity

288 to voxel size (see the differences among Figures 6e–h) and the variation of cubic root of Vcdp
 289 substantively counterbalance the variation of cubic root of Ve owing to their homogeneity. These
 290 two reasons together improve the robustness of 3DRED.
 291

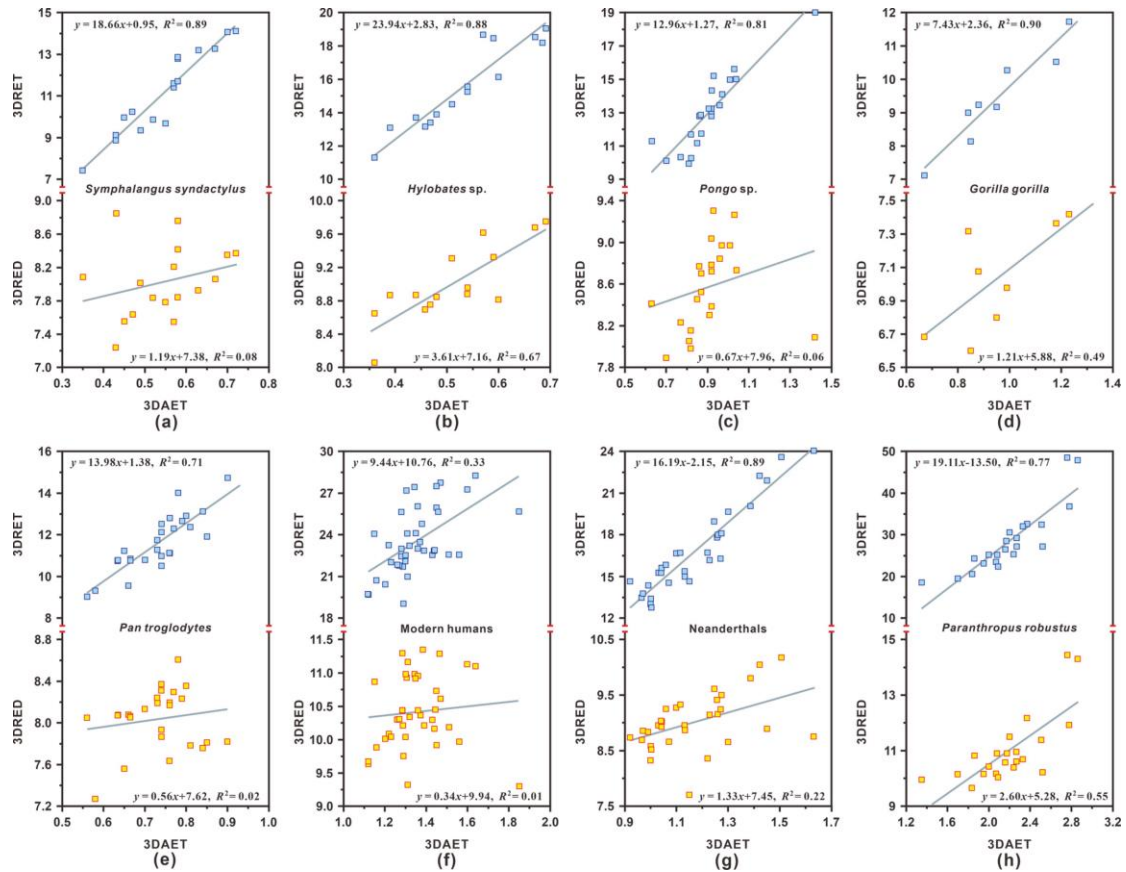


292
 293 FIGURE 6. The sensitivity of four parameters to voxel size, including (a) enamel volume, (b)
 294 enamel–denture junction (EDJ) surface area, (c) cubic root of coronal dentine volume, and (d) cubic
 295 root of enamel volume. The first two parameters (a,b) affect the result of three - dimensional
 296 average enamel thickness (3DAET), the first three (a - c) for three - dimensional relative enamel
 297 thickness (3DRET), and the last two (c,d) for three - dimensional ratio of enamel - thickness to
 298 dentine - thickness (3DRED). For these four parameters, their relative errors varying with voxel
 299 size are shown below in figures (e–h), respectively.

300
 301 Another question is why there exists threshold voxel size. A possible explanation is that when voxel
 302 size gets larger, the small parts (e.g., dentine horn tip and small fissures) in the tooth could be over
 303 simplified or even melted down, thus causing measurement deviation. It is necessary to mention
 304 that the threshold voxel size repeated above (~40 µm) is only relevant for the sample studied here
 305 (NX - C2 - 9). It is most likely that the threshold voxel size will be different from 40 µm for other
 306 larger (e.g., Gorilla) or smaller (e.g., Hylobates) hominid teeth due to the size and structure
 307 differences from sample to sample.

309 3.2 Correlation between 3DAET and 3DRET, and between 3DAET and 3DRED

310 To investigate the relationship between 3DRET and 3DAET and the relationship between 3DRED
 311 and 3DAET, enamel thickness measurements for a total of 179 M were analyzed and the results are
 312 detailed in full in Supplementary Material Table 2. Figure 7 presents the results for eight hominid
 313 genera. For all taxon except modern humans, 3DRET is correlated with 3DAET by linear
 314 relationship. The regression coefficients are close to 0.8 or above in most cases, indicating that
 315 3DRET is not an independent variable with respect to 3DAET. In contrast, 3DRED shows less
 316 degree of correlation with 3DAET, with R2 smaller than 0.5 in most cases. Thus, a question arises:
 317 Why there exists a linear relationship between 3DAET and 3DRET? As shown in Equation (2),
 318 there are three parameters involved in the calculation of 3DRET: Ve, Sedj, and cubic root of Vcdp.
 319



320

321 FIGURE 7. The relationship between three - dimensional relative enamel thickness (3DRET) and
 322 three - dimensional average enamel thickness (3DAET), and between three - dimensional ratio of
 323 enamel - thickness to dentine - thickness (3DRED) and 3DAET for (a) *Symphalangus syndactylu*,
 324 (b) extant *Hylobates*, (c) extant *Pongo*, (d) *Gorilla gorilla*, (e) *Pan troglodytes*, (f) modern humans,
 325 (g) Neanderthals, and (h) *Paranthropus robustus*. All teeth are mandibular molars. In each figure,
 326 the upper part shows the relationship between 3DRET and 3DAET, while the lower part shows the
 327 relationship between 3DRED and 3DAET

328 For specific taxa (genus or species), the variation of V_e and S_{edj} exist between different samples,
 329 but the variation of cubic root of V_{cdp} may be very small, if the coronal dentine volume differences
 330 are not large enough. For instance, the ranges of V_e , S_{edj} , and cubic root of V_{cdp} for Neanderthals
 331 ($n = 31$) can be expressed as 252.78 ± 43.72 (mean and SD), 219.67 ± 40.74 , and 7.01 ± 0.45 ,
 332 respectively. Compared to the ranges of V_e and S_{edj} , the range of cubic root of V_{cdp} is much smaller.
 333 Under this condition, the three parameters bear uneven influences on 3DRET, and cubic root of
 334 V_{cdp} can be approximately regarded as a constant. Therefore, Equation (2) can be reformulated as
 335 Equation (6).

$$3DRET \approx 100 \times \frac{V_e / S_{edj}}{a} + b \approx 100 \times \frac{3DAET}{a} + b$$

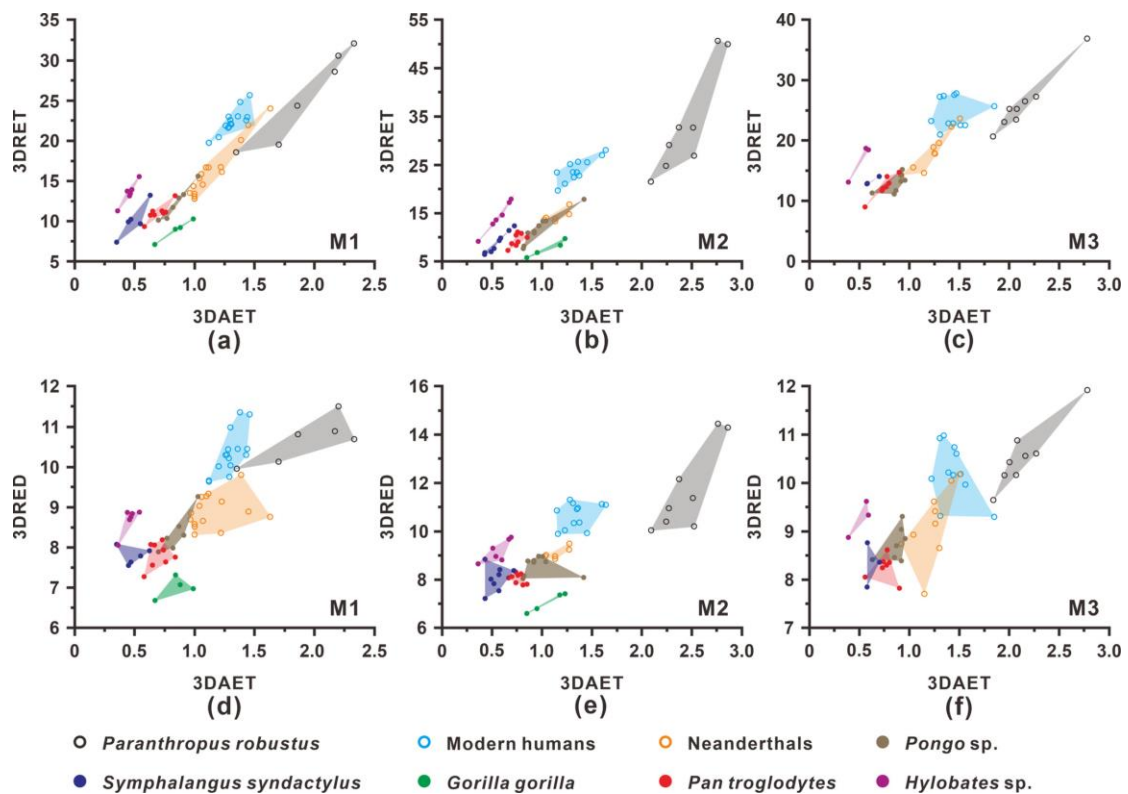
336

337 (6)

338 where a and b are constants that related to the taxonomic affinity of the studied tooth.

339 As we can see in Figure 7g, 3DRET shows an evident linear relationship with 3DAET (Neanderthals,
 340 $R^2 = .89$), which is consistent with Equation (6). Compared to other primates, modern humans have
 341 reduced crown size with respect to their body size, in relation with the drastic and accelerated

342 reduction of the face that occurred in modern humans since the end of the Late Pleistocene (Brace,
 343 Rosenberg, & Hunt, 1987; Macchiarelli & Bondioli, 1986). During this recent evolutionary phase,
 344 allometric reorganization in enamel and dentine proportions may have occurred in modern humans
 345 (Grine, 2005). This could explain why modern humans show such a strange relationship (Figure 7f,
 346 not linear) between 3DRET and 3DAET compared with other hominids. It is necessary to mention
 347 that no guarantee can be given that Equation (6) is valid for all species. It depends on the relative
 348 variations (i.e., the ratio of SD to mean) of V_e , S_{edj} , and cubic root of V_{cdp} . However, the
 349 phenomenon that the linear correlation between 3DRET and 3DAET is fairly common in our study
 350 samples (Figure 7). This phenomenon will lead to two consequences. First, it is not practicable to
 351 use bivariate plot of 3DRET and 3DAET (just like traditional bivariate plot of the mesiodistal and
 352 buccolingual diameters) to offer diagnostic information for specimen with uncertain taxonomic
 353 affinity, because the two variables would probably form a line (Figure 8a–c) but not define a
 354 discriminative polygon. Curiously, the usage of bivariate plot of 3DRET and 3DAET are really rare
 355 in previous studies. Possibilities for that include the linear relationship between 3DRET and 3DAET.
 356 Second, discriminant information could be double counted, if both 3DAET and 3DRET are used to
 357 diagnosis the taxonomic status of a given tooth. For example, Zanolli, Kullmer, et al. (2019) utilized
 358 adjusted Z - score statistics to assess the taxonomy of Indonesian fossil hominid and compared both
 359 3DAET and 3DRET to that of other fossil and extant hominid, including Pongo, Gigantopithecus
 360 blacki, Homo erectus/ergaster, Homo erectus, Lufengpithecus, Sivapithecus, modern humans, and
 361 Neanderthals. In their supplementary figure 20, 3DAET and 3DRET show similar pattern and for
 362 some samples (e.g., Arjuna 9 LM2, SMF - 8855, and SMF - 8865), the results are even overlapped.
 363 On account of the high similarity between the pattern of 3DAET and 3DRET, it is plausible that one
 364 of them is likely redundant in the sense of taxonomic assessment.
 365



366
 367 FIGURE 8. The taxonomic bivariate plot of three - dimensional relative enamel thickness (3DRET)

<i>Pa. rob.</i>							0.269	
Second molars								
<i>Gorilla</i>								
<i>Sympha.</i>	0.44		0.895					
<i>Pan</i>	0.064	0.402						
<i>Pongo</i>								
<i>Hylobates</i>				0.099		0.873		
Nean.					0.873			
Mo. hu.								0.143
<i>Pa. rob.</i>								
Third molars								
<i>Gorilla</i>		-	-	-	-	-	-	-
<i>Sympha.</i>	-		0.569	0.138		0.091		
<i>Pan</i>	-	0.425						
<i>Pongo</i>	-	0.909	0.798		0.053	0.097		
<i>Hylobates</i>	-	0.127	0.053	0.138		0.735	0.052	
Nean.	-				0.612			
Mo. hu.	-							0.621
<i>Pa. rob.</i>	-						0.97	

401

402 ^aNote: *Sympha.* = *Symphalangus syndactylus*. Nean. = Neanderthals. Mo. hu. = Modern humans.

403 *Pa. rob.* = *Paranthropus robustus*.

404 Abbreviations: 3DRED, three - dimensional ratio of enamel - thickness to dentine - thickness;

405 3DRET, three - dimensional relative enamel thickness.

406 a Blank cell indicates significant differences ($p < .05$). A hyphen indicates no molars of that position
407 of that taxon.

408

409 4 CONCLUDING REMARKS

410 Compared to 3DRET, 3DRED shows some advantages. Specifically, 3DRET is sensitive to voxel
411 size while 3DRED is more robust. Besides, 3DRET shows a linear link to 3DAET in a considerable
412 number of cases, probably causing information redundancy during taxonomic assessments. In
413 contrast, 3DRED shows less correlation with 3DAET, so that they can be used in combination in
414 multivariable - based statistics. Furthermore, 3DRED shows more taxonomic value compared to
415 3DRET in a large sample size. Despite the significance of 3DRED, it does not mean that this index
416 could replace 3DRET, especially considering the important role of 3DRET in dietary reconstruction.
417 Under certain conditions, 3DRED is promising to be a robust and reliable alternative to 3DRET in
418 taxonomic study. These conditions mainly include: (a) the tooth sample is scanned at relatively low
419 spatial resolution, or (b) 3DRET needs to be coupled with 3DAET (like the 3DRET - 3DAET
420 bivariate plot or adjusted Z - score statistics with both 3DRET and 3DAET included) to deduce the
421 taxonomic status of a given sample.

422

423 ACKNOWLEDGMENTS

424 For access to the micro - CT image stacks of hominid tooth, the authors thank the following
425 institutions: University of Liege (Belgium); Evolutionary Anthropology, Duke University (Durham,

426 NC); Musée des Confluences, Lyon, Centre de Conservation et d'Étude des Collections (France);
427 Croatian Natural History Museum (Croatia); Musée des Beaux - Arts d'Angoulême (France);
428 Thüringisches Landesamt für Archäologische Denkmalpflege mit Museum für Ur - und
429 Frühgeschichte (Germany); Institut für Ur - und Frühgeschichte, Universität Nürnberg - Erlangen
430 (Germany). For scanning and technical assistance, the authors thank Zonglin Wu, Binhong Wan,
431 Yunfei Zhu, and Qiaoli Xu. The authors sincerely appreciate two anonymous reviewers for their
432 constructive comments and suggestions. The authors sincerely appreciate the beneficial discussions
433 with Prof Yongbiao Wang. This study was supported by the funds from the National Natural Science
434 Foundation of China (grant Nos. 40772011 and 41572023), and by a grant of the Bagui Scholar of
435 Guangxi.

436

437 CONFLICT OF INTEREST

438 The authors declare no conflict of interest.

439

440 AUTHOR CONTRIBUTIONS

441 Zhixing Yi: Conceptualization; methodology; validation; writing - original draft; writing - review
442 and editing. Wei Liao: Investigation; validation; writing - original draft; writing - review and
443 editing. Clément Zanolli: Methodology; writing - original draft; writing - review and editing. Wei
444 Wang: Conceptualization; funding acquisition; investigation; validation; writing - original draft;
445 writing - review and editing.